Surface-Enhanced Raman Scattering by Molecules Adsorbed on Aqueous Copper Colloids

J. A. Creighton,† M. S. Alvarez, D. A. Weitz,* S. Garoff, and M. W. Kim

Exxon Research and Engineering Company, Linden, New Jersey 07036 (Received: February 10, 1983)

Aqueous copper colloids prepared by borohydride reduction of Cu^{2+} solutions are shown by dynamic light scattering to aggregate in the presence of pyridine. Aggregation is accompanied by the appearance of a broad extinction band in the red region, and these aggregated colloids show enhanced Raman scattering by adsorbed pyridine or other adsorbates for excitation at 647.1 nm or longer wavelengths. The Raman enhancement factor for a typical colloid at 647.1 nm is measured to be 1.5×10^5. The steep rise in the Raman excitation profile toward the red is shown to be associated with the rise in $|\epsilon|^2$ for copper toward longer wavelengths. The frequencies and relative intensities in the adsorbed pyridine spectrum are discussed in terms of the orientation of the molecule with respect to the surface and the potential across the colloid–aqueous interface. Preliminary Raman measurements of competitive exchange equilibria between pyridine and other adsorbates are presented.

Introduction

Particles of the copper, silver, and gold group of metals are notable in showing strong, electronic plasma resonances in the visible region, as a result of which colloidal dispersions or island films of these metals have distinct colors. The wavelengths of these resonances, which are in large part determined by the dielectric function of the metals, depend also on the size and shape of the particles and on their proximity to each other, and thus the colors of the colloids vary depending on the method of preparation and on the state of aggregation. These resonances and the similar resonances localized on bumps or cavities of roughened bulk surfaces of these metals, are believed to make a major contribution to the surface-enhanced Raman (SER) scattering by molecules adsorbed on these surfaces.[1] This has been demonstrated particularly clearly by measurements on silver or gold colloids[2,3] or on silver island films,[4] which show that if the adsorption spectrum is changed by aggregating the colloids or by increasing the thickness of a dye coating on the island films there is a related change in the surface Raman excitation profiles.

Although SER scattering with high intensity has been reported for roughened bulk copper[5-8] as well as from silver and gold surfaces, there has been no previous report of SER scattering from molecules adsorbed on copper colloids. Copper colloids are considerably more sensitive to oxidation than those of silver or gold, yet there are several reports, going back to the first decade of this century, of the preparation of copper sols by reduction of solutions of copper salts or by other methods.[9] This paper reports the first observation of surface-enhanced Raman scattering by various molecules adsorbed on copper sols, prepared by borohydride reduction of aqueous solutions of Cu^{2+} ions and with appropriate chemical measures taken to provide adequate stability against oxidation and precipitation. Aggregation of the colloids was investigated in situ by dynamic light scattering and absorption spectroscopy and in this work, we use the SER spectra and excitation profiles of copper colloids to gain insight into the origins of the enhancement as well as to investigate the nature of the adsorption of pyridine at the copper–aqueous interface. Some preliminary SER data illustrating the application of Raman spectroscopy for studying adsorbate exchange are also presented.

Experimental Section and Results

Preparation of Colloids. Aqueous solutions of copper(II) sulfate (2×10^{-2} M, 5 mL) and pyridine (1×10^{-3} M, 10 mL) were added to a trisodium citrate solution (2.8×10^{-3} M, 60 mL). To this was added 30 mL of a freshly prepared 2×10^{-2} M solution of sodium borohydride in 1.9×10^{-2} M sodium hydroxide. All solutions were prepared with high-purity water, and all glassware had been soaked in chromic acid and further rinsed in 1 M hydrochloric acid, followed by thoroughly rinsing in pure water. The colloid, which on mixing was pale yellow-brown, darkened over the course of 5–10 min becoming grey-brown, due to aggregation (see discussion on absorption spectra below). The considerable excess of borohydride in the sol was used to provide a buffer against oxidation of the copper particles, and the high pH served to increase the life of the borohydride ions, while the citrate ions stabilized the colloid against precipitation. In stoppered cells the colloid was stable for over 24 h, though in inadequately cleaned glassware slow decomposition of borohydride ions occurred, giving bubbles of hydrogen on the surface of the glass.

This grey-brown colloid showed intense Raman scattering by adsorbed pyridine on excitation at 647.1 nm or longer wavelengths. Use of the same concentrations and amounts of reagents except for the omission of pyridine gave a copper colloid which remained yellow-brown. On addition of pyridine solution (1×10^{-3} M, 10 mL, to 95 mL of colloid) the colloid quickly became grey-brown, however,

† Chemical Laboratories, University of Kent, Canterbury CT2 7NH, England.

(1) See, for example, "Surface Enhanced Raman Scattering", R. K. Chang and T. Furtak, Ed., Plenum, New York, 1982.
(2) J. A. Creighton, C. G. Blatchford, and M. G. Albrecht, *J. Chem. Soc., Faraday Trans. 2*, 75, 790 (1979).
(3) C. G. Blatchford, J. R. Campbell, and J. A. Creighton, *Surf. Sci.*, 120, 435 (1982).
(4) D. A. Weitz, S. Garoff, and T. J. Gramila, *Opt. Lett.*, 7, 168 (1982).
(5) B. Pettinger and H. Wetzel, *Ber. Bunsenges.* Phys. Chem., 85, 473 (1981).
(6) C. S. Allen, G. C. Schatz, and R. P. Van Duyne, *Chem. Phys. Lett.*, 75, 201 (1980).
(7) M. L. A. Temperini, H. C. Chagas, and O. Sala, *Chem. Phys. Lett.*, 79, 75 (1981).
(8) I. Pockrand, *Chem. Phys. Lett.*, 85, 37 (1982), and references therein.
(9) "Handbuch der anorganischen Chemie", 60, Teil A2, Gmelin-Institut, 8 Aufl, 1955, pp 718–25.

0022-3654/83/2087-4793$01.50/0

TABLE I: Raman Frequencies, Relative Intensities, Depolarization Ratios, and Assignments for Pyridine Adsorbed on a Copper Sol

copper colloid					aqueous pyridine solution	
	rel int					
freq, cm^{-1}	647.1 nm	752.5 nm	depol ratio	assgn[a]	freq, cm^{-1}	rel int
244	10			ν(Cu-N)		
386	0.5	0.14	~1	a_2	385	0.2
416	3	3	0.48	b_1	411	0.8
632	37	38	0.46[b]	a_1	618	2
649	0.8			b_2	654	6
695	0.8			b_1	708	0.2
753	0.8			b_1	760	0.2
941	0.8			b_1	948	0.5
1010	100	100	0.44[b]	a_1	1002	100
1037	1.5			a_1	1036	58
1065	2.5			a_1, b_2	1071	2
1150	0.5	0.06		b_2	1153	1.5
1212	61	35	0.45[b]	a_1	1220	7
1236	0.5			b_2	1232	1
1261	0.5					
1442	0.8		0.78	b_2	1444	0.4
1477	1		0.65	a_1	1487	2
1566	1			b_2	1576	6
1593	43	29	0.50[b]	a_1	1593	7
1641	1.5					
3030	0.5			$3a_1 + 2b_2$	3070	97

[a] Referred to free pyridine (C_{2v}) asssignments of ref 21. [b] Aqueous pyridine solution depolarization ratios: 618 (0.75); 1002 (0.03); 1220 (0.58); 1593 (0.56).

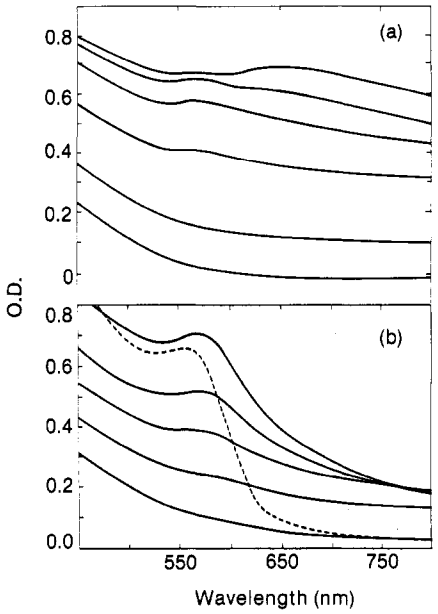

Figure 1. Full lines show the increasing optical density (0.5 cm thickness) during the formation of copper colloids (a) without pyridine and (b) containing 1×10^{-4} M pyridine: (a) 7, 13, 22, 40, 108 min; and (b) 2, 7, 10, 15, 21, 68 min after the start of reduction of Cu^{2+}. (---) is the calculated optical density for a dispersion of 20-nm-diameter copper spheres in water from Mie theory.

and this colloid also exhibited intense surface-enhanced Raman scattering upon excitation in the red. The extinction spectras of these grey-brown and yellow-brown forms, showing the evolution of the extinction as the colloids develop, are given in Figure 1.

Copper colloids containing the other adsorbates 4,4′-bipyridine, benzotriazole, thiophenol, diphenyl sulfide, and triphenylphosphine were also prepared, either by adding the adsorbate before or after the reduction by borohydride or by displacing adsorbed pyridine from a grey-brown copper–pyridine sol. The colloids were of rather variable stability with respect to precipitation, and precipitation was usually rapid at adsorbate concentrations $>1 \times 10^{-4}$ M. The latter method of pyridine displacement gave the colloids of the most reproducible stability and showing the most intense Raman scattering. The sparingly water-soluble substances, PhSH, Ph_2S, and Ph_3P, were added to the colloids as 1×10^{-3} M solutions in 50% aqueous propan-2-ol.

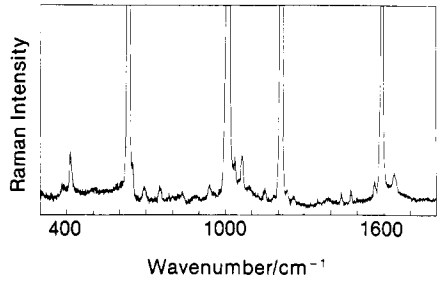

Figure 2. The Raman spectrum of pyridine (1×10^{-4} M) adsorbed on a grey-brown copper sol: 647.1-nm excitation (460 mW), bandpass 1 cm^{-1}, count time 1 s per cm^{-1}, 8 scans.

Raman Scattering. Figure 2 shows the Raman spectrum of a typical copper–pyridine sol obtained by using 647.1-nm excitation. All of the bands are due to adsorbed pyridine, and the spectrum shows almost the full set of pyridine Raman bands, some of which are intrinsically weak. The frequencies of the bands and the relative intensities and depolarization ratios are given in Table I. The relative intensities of the strongest bands were reproducible to within ±7% for different sols with the same excitation wavelength but, as Table I shows, there was a distinct difference between the intensities of the bands at 1212 and 1593 cm^{-1}, and also of some of the non-a_1 bands, relative to the 1010-cm^{-1} band for 647.1-nm excitation and for excitation at 752.5 nm. As was observed for silver and gold colloids,[2,3] and also for molecules adsorbed at electrodes,[10] the depolarization ratios of all the strong a_1 bands are close to 0.5, in contrast to pyridine in solution for which these bands have a wider range of values, both less than and

(10) D. L. Jeanmaire and R. P. Van Duyne, *J. Electroanal. Chem.*, 84, 1 (1977).

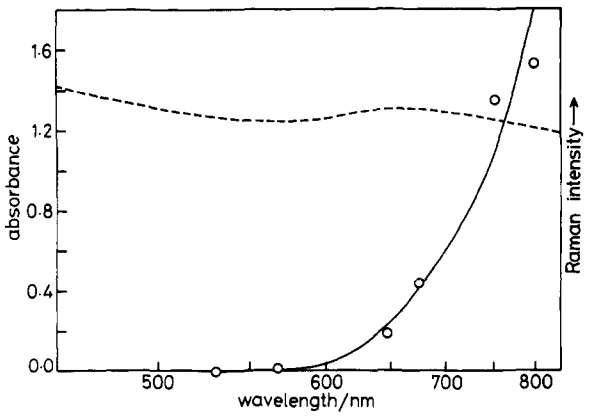

Figure 3. Raman excitation profile (—) of the 1010-cm^{-1} band of pyridine adsorbed on a copper colloid, showing the experimental points superimposed on a curve calculated from the absorption (taken to equal the extinction) by means of eq 1. (---) is the extinction spectrum of the colloid.

greater than 0.5 (see Table I). However, some of the weaker SER bands corresponding to a_2 and b_2 modes had depolarization ratios substantially greater than 0.5, as shown in Table I.

A conspicuous feature of Figure 2, and also the SER spectra of pyridine adsorbed at copper–aqueous electrodes[5-7] or at low-temperature copper–vacuum interfaces,[8] is the high intensity of the 632-, 1212-, and 1593-cm^{-1} bands relative to the band at 1010 cm^{-1}, and the low relative intensities of all other bands, including 1037 cm^{-1}. In contrast, for pyridine at silver or gold surfaces 1037 cm^{-1} is a rather prominant band. The pyridine frequencies for all of these surfaces are characteristic of pyridine chemisorbed to the metal, as is shown particularly by the 1003- and 618-cm^{-1} bands of aqueous pyridine which are well documented[11] to shift to higher frequencies (1010 and 632 cm^{-1} for the copper sols) on forming pyridine complexes with metal ions. Also clearly indicative of chemisorbed pyridine in the copper colloid is the band due to Cu–N stretching at 244 cm^{-1}. Although bands in this frequency region for pyridine adsorbed at silver electrodes in the presence of chloride ions have been assigned either to Ag–N[12] or to Ag–Cl stretching,[13] in the absence of chloride ions in the copper colloids this band is clearly due to Cu–N stretching.

It is further of note that, although the SER spectra of the copper–pyridine sols and of pyridine adsorbed at copper electrodes at −0.6 V (SCE)[7] are similar, the frequencies of all the pyridine modes are slightly less for the colloids than for the electrodes, the difference being greatest for the strong band near 1600 cm^{-1}. Temperini et al.[7] have shown that there is a decrease in the SER frequencies of pyridine at copper electrodes on changing the electrode potential from −0.5 to −1.1 V, and the ca. 1600-cm^{-1} band is the most sensitive to change in potential. The difference of frequencies between the colloids and electrodes may therefore be a consequence of the strongly negative potential of the sol particles in the strongly reducing environment. The potential of the particles, viewed as microelectrodes, may be estimated by means of the

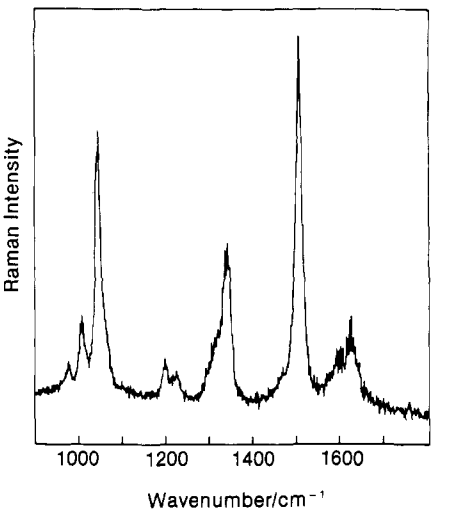

Figure 4. Raman spectrum of 4,4′-bipyridyl (1×10^{-3} M) adsorbed on a copper sol: 647.1-nm excitation.

Nernst equation from the composition of the sol and the standard reduction potential for the half-reaction

$$H_2BO_3^- + 5H_2O + 8e^- \rightleftharpoons BH_4^- + 8OH^-$$
$$E_0 = -1.48 \text{ V (SCE)}$$

If we assume the only source of oxidation of BH_4^- to be the initial $CuSO_4$ the potential of the particles is thus calculated to be −1.36 V, while if we assume 90% decay of the excess BH_4^- the potential is calculated to be −1.34 V. It is therefore concluded that the potential of the colloid particles is considerably more negative than that of the electrode, consistent with their lower pyridine frequencies.

The Raman excitation profile for the 1010-cm^{-1} pyridine band of a grey-brown copper sol was measured relative to the 1002-cm^{-1} band of a 10% aqueous pyridine solution, and is shown in Figure 3 together with an extinction spectrum of the same sol. For these measurements, absorption of the scattered light was minimized by using near-grazing incidence of the input laser to the cell window facing the spectrometer, and the intensities plotted in Figure 3 were corrected for absorption of the incident light by the colloid. Raman intensity measurements were commenced 80 min after preparing the sol, and during the time of the measurements (~100 min) there was a decay in the extinction of 10% throughout the range 500–800 nm, with no change in the shape of the extinction curve. The decay in the SER intensity measured with 752.5-nm excitation was 19%, and a small correction was therefore made to the intensities in Figure 3, assuming the decay to be linear. A repeat of the measurements with another similar sol, commencing 160 min after preparing the sol, yielded an almost identical excitation profile. A further similar sol was used to measure the SER enhancement factor for the 1010-cm^{-1} band for 647.1-nm excitation by comparing the Raman intensity with that of the 1003-cm^{-1} band of a 20% aqueous pyridine solution. The amount of adsorbed pyridine was determined by difference from the total pyridine concentration in the sol by sedimenting the sol particles by ultracentrifugation and measuring the nonadsorbed pyridine concentration in the supernatant by ultraviolet spectrophotometry.[3] The enhancement factor for 647.1-nm excitation after correcting for laser light absorption by the colloid was thus found to be 1.5 (±0.2) × 10^5, comparable to the enhancement factor measured by an analogous procedure for a well aggregated gold sol of 3×10^5.[3]

(11) A. T. Hutton and D. A. Thornton, *Spectrochim. Acta, Part A*, **34**, 645 (1978); S. Suzuki and W. J. Orville-Thomas, *J. Mol. Struct.*, **37**, 321 (1977), and references therein.

(12) J. A. Creighton, M. G. Albrecht, R. E. Hester, and J. A. D. Matthew, *Chem. Phys. Lett.*, **55**, 55 (1978); J. R. Lombardi, E. A. Shields Knight, and R. L. Birke, *Ibid.*, **79**, 214 (1981).

(13) H. Wetzel, H. Gerischer, and B. Pettinger, *Chem. Phys. Lett.*, **78**, 392 (1981); H. Wetzel and H. Gerischer, *Ibid.*, **76**, 460 (1980); R. L. Garrell, K. D. Shaw, and S. Krimm, *J. Chem. Phys.*, **75**, 4155 (1981).

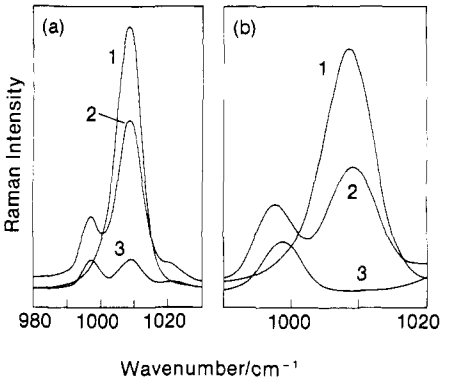

Figure 5. Raman spectra showing competitive adsorption on copper sols by pyridine and (a) diphenyl sulfide and (b) thiophenol. Total pyridine concentration 1×10^{-4} M; concentrations of diphenyl sulfide: [1], 0.0; [2], 7×10^{-5} M; [3], 2×10^{-4} M; concentrations of thiophenol: [1], 0.0; [2], 1×10^{-5} M; [3], 3×10^{-5} M, 647.1-nm excitation.

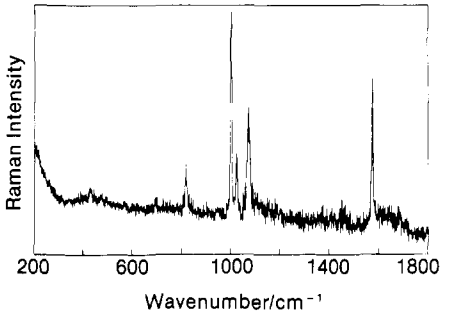

Figure 6. Raman spectrum of thiophenol (3×10^{-5} M) adsorbed on a copper colloid, 647.1-nm excitation.

SER spectra of colloids containing adsorbates other than pyridine were also obtained. Figure 4 shows the SER spectra of 4,4′-bipyridine adsorbed on a copper sol, prepared by adding 4,4′-bipyridine (0.01 M in 10% aqueous propan-2-ol, 1 mL) to 10 mL of a pyridine-free copper sol. Similarly adding triphenylphosphine (1×10^{-3} M in 50% aqueous propan-2-ol, 0.5 mL) to 10 mL of copper colloid enabled a spectrum of adsorbed triphenylphosphine to be obtained, with principal bands (relative intensities) at 1090 (25), 1026 (40), 997 (100), and 984 (shoulder) cm^{-1}. Both of these colloids darkened to grey-brown as on adding pyridine, but began to precipitate in about 30 min. Triphenylphosphine, diphenyl sulfide, and benzotriazole appear to have similar binding affinities for the sol particles as pyridine, since adding any of these ligands in aqueous propan-2-ol to a copper–pyridine sol so that the new adsorbate concentration was ca. 3×10^{-5} M gave SER spectra consisting of a superposition of bands of adsorbed pyridine and of the new adsorbate. In contrast the much stronger adsorbate thiophenol at 3×10^{-5} M completely displaced adsorbed pyridine. SER spectra comparing the ability of diphenyl sulfide and thiophenol to displace adsorbed pyridine, and illustrating the potential of SER spectroscopy for investigating metal–aqueous adsorption equilibria, are presented in Figure 5, while Figure 6 shows a SER spectrum of adsorbed thiophenol over a wider frequency range.

Dynamic Light Scattering and Electron Microscopy. Samples of colloids were prepared for transmission electron microscopy by evaporating very small volumes of the colloids in air. The yellow-brown pyridine-free sol appeared from the micrographs to be essentially unaggregated, while there was considerable aggregation in the case of the grey-brown copper–pyridine sol, but the quality of the images was extremely poor, due probably to oxidation of the copper particles on exposure to air. Dynamic light scattering was therefore used to determine the particle size and to monitor the aggregation of the particles in situ in the sols.

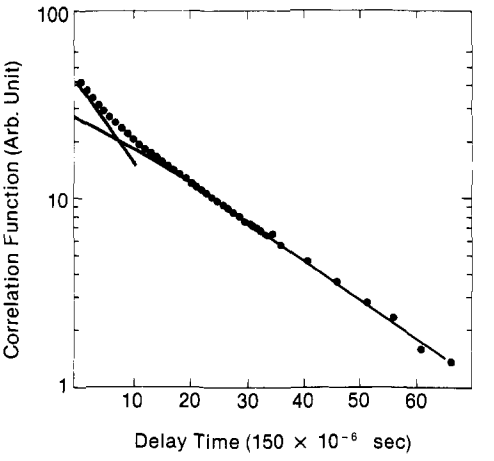

Figure 7. Typical correlation function of copper colloid, fit to a double exponential decay (solid line).

Standard experimental techniques were used to measure the autocorrelation function of the quasi-elastically scattered light.[14] The concentration fluctuations of the copper colloids decay exponentially with time due to diffusion, so that the autocorrelation function contains an exponential term with a decay rate $2DK^2$, where K is the magnitude of the scattering vector. The diffusion constant, D, is related to the hydrodynamic radius of the colloid particles, R_H, by the Stokes–Einstein relation

$$D = \frac{kt}{6\pi\eta R_H}$$

where k is Boltzmann's constant, T the temperature, and η the solvent viscosity. Thus a determination of the diffusion constant from the autocorrelation function gives a measure of the hydrodynamic radius of the sol particles. The duration time of each experiment was several minutes for the colloids without pyridine, and ca. 30 s for the samples containing pyridine. A sequence of measurements was taken as the colloids matured after their preparation in order to monitor the growth and aggregation of the particles.

None of the correlation functions measured could be fitted well with a single exponential decay. A typical example of this behavior is shown in Figure 7. We believe this behavior is an indication of one of the following: (1) a polydispersity in the size of the colloidal particles leading to a distribution of mean radii; (2) the existence of nonspherically shaped particles which would result from the aggregation of the individual spherical particles into random chains, and would yield more than one radius corresponding to their effectively ellipsoidal shape; or (3) the fluctuations of both the aggregated particles as a whole and of the individual spheres that comprise the aggregates, resulting in two different decay times. While we believe the most likely cause of the behavior is the first, or a combination of the first and second reasons (polydispersity and nonsphericity), to properly distinguish between these two possibilities requires an additional measurement of the autocorrelation function at a different scattering vector. Unfortunately, the relatively rapid changes that occurred as the colloid matured precluded an accurate measurement

(14) B. Berne and R. Pecora, "Dynamic Light Scattering", Wiley, New York, 1976.

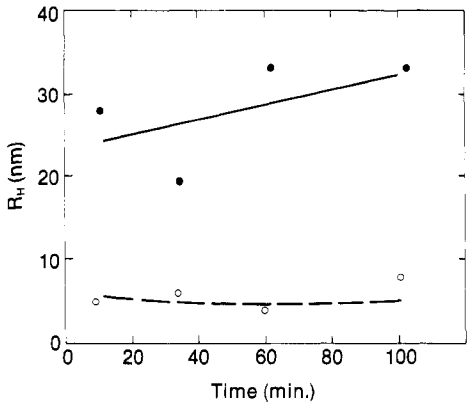

Figure 8. Characteristic hydrodynamic radii of copper colloid without pyridine as a function of maturation time. The two sets of points refer to the two radii determined from the correlation decay function, as discussed in the text.

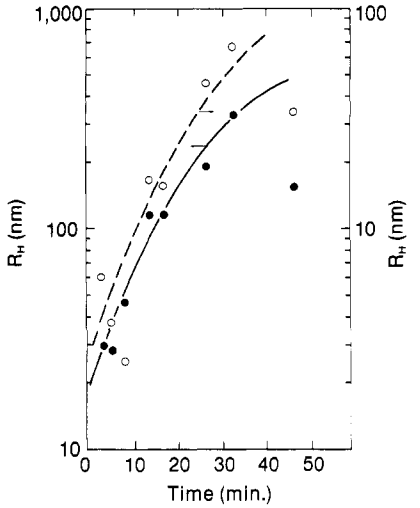

Figure 9. Characteristic hydrodynamic radii of copper colloid with 1 × 10^{-4} M pyridine added as a function of maturation time of the colloid. The two sets of points refer to the two hydrodynamic radii determined from the correlation decay function, as discussed in the text. The solid points are the larger radii while the open points are the smaller radius.

of the correlation function at two different scattering vectors with the same state of colloid maturation and with the single detector used in these experiments.

However, considerable insight can be gained by assuming a double exponential decay, which results in a reasonable fit to the data as shown in Figure 7. We take the two resulting values of D to reflect two mean hydrodynamic radii characteristic of the colloid. The mean particle sizes thus determined are shown as a function of time as the colloid matures for a colloid prepared without pyridine in Figure 8, and for one prepared with pyridine in Figure 9. Both colloids show two mean radii with this procedure, and the initial R_H of each are roughly comparable, being ~5 and ~30 nm for the small or large radii, respectively. Subsequently, the size of the colloid prepared without pyridine remains constant over the course of the measurements (~100 min) as shown in Figure 8. In contrast, the colloid prepared with pyridine grows rapidly and substantially in both dimensions in the course of experiments, as shown in Figure 9, and reaches an ultimate radius of several hundred nanometers. Despite the possible ambiguities in the precise interpretation of the data, it is clear that the mean particle dimensions of the colloids prepared with pyridine are substantially greater than those of the colloids prepared without pyridine.

The picture that emerges is thus totally consistent with the interpretation that the copper particles comprising the colloids are of average diameter ca. 5 nm. There is a very small amount of aggregation for the colloid without pyridine, resulting in some of the particles having a characteristic dimension of ~25–30 nm. In contrast, for the colloids prepared with pyridine, there is substantial aggregation which results in a mean hydrodynamic radius which grows in time and has a value of several hundred nanometers. We note that the nature of this behavior is quite similar to that observed for the SER-active gold colloids.[3]

Discussion

Extinction Spectra and Aggregation. The experimental extinction spectra of the pyridine-free copper sol are compared in Figure 1a with a spectrum calculated by means of Mie theory for an aqueous dispersion of isolated small copper spheres with the same total copper concentration as in the experimental sol. The optical constants of copper were those of Hagemann et al.[15] The extinction is independent of particle size for a given mass concentration in the dipole approximation, and thus the sphere diameter, taken to be 20 nm, is not a critical quantity provided it is much less than the optical wavelength. The calculated curve is seen to reproduce fairly well the extinction spectrum of the final sol, notably in the wavelength of the dipole plasma resonance at 560 nm and in the optical density over the range 450–550 nm. As has already been shown for copper particles,[16] a departure from spherical shape results in a shift of the plasma resonance to longer wavelenghts together with a substantial increase in the peak absorbance, and thus comparison of the calculated and measured extinction spectra in Figure 1a supports the conclusion from the dynamic light scattering measurements that the yellow-brown colloid consists mainly of unaggregated spherical particles with diameters much less than the wavelength. The larger optical density measured in the 600–850-nm range compared to that calculated for isolated spheres (Figure 1a) may be due to a small degree of aggregation in the pyridine-free sol (cf. Figure 1b, and discussion below) as indicated by the dynamic light scattering results. Published Mie calculations[17] also reproduce quite well the evolution of the extinction spectrum in Figure 1a as the colloid particles nucleate and grow. These calculations show that for particles less than ca. 5 nm in diameter the plasma resonance is flattened and shifted slightly to longer wavelengths, due to the increased damping of the resonance as a result of the additional scattering of the electrons in wall collisions.

The dynamic light scattering results clearly show that on adding pyridine the yellow-brown copper colloid is induced to aggregate. As is well established,[18] the effect of the close proximity of spheres within particle aggregates is to shift the plasma resonance to longer wavelengths due to coupling between the plasma modes of neighboring spheres, thus changing the extinction spectrum. This effect is clearly seen on comparing the spectra of the sols with and without pyridine in Figure 1, where the coupled plasma mode of the aggregates in the grey-brown sol (Figure 1b) is seen as a broad band on the long wavelength

(15) H. J. Hagemann, W. Gudat, and C. Kunz, *J. Opt. Soc. Am.*, **65**, 742 (1957); Report SR-74/7, Deutches Elektronen-Synchrotron, 2 Hamburg 52, Notkestieg 1.

(16) D.-S. Wang and M. Kerker, *Phys. Rev. B*, **24**, 1777 (1981).
(17) S. Garoff and C. D. Hanson, *Appl. Opt.*, **20**, 758 (1981).
(18) J. C. Maxwell-Garnett, *Phil. Trans.*, **203**, 385 (1904); R. Clippe, R. Evrard, and A. A. Lucas, *Phys. Rev. B*, **14**, 1715 (1976).

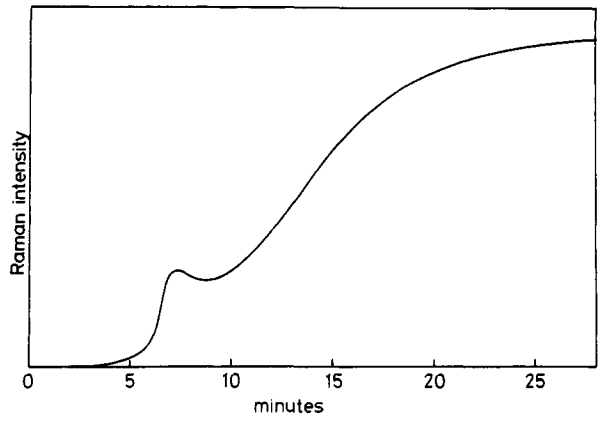

Figure 10. Evolution of the intensity of the 1010-cm^{-1} Raman band of adsorbed pyridine during the formation of the copper sol of Figure 1b, 647.1-nm excitation.

side of the 560-nm single-sphere band, the intensity of this broad absorption increasing as the aggregation proceeds. The effect of pyridine on the copper sols is thus similar to its aggregating effect on silver and gold sols.[2,3] Figure 1 shows that even in the very early stages of formation of the colloids, there is significantly greater absorption in the red region for the sol containing pyridine, consistent with a greater degree of aggregation already at this early stage.

Raman Scattering. In the case of silver and gold sols there is strong evidence that aggregation is essential for the colloids to show high SER intensity, the pyridine band intensity for example increasing progressively from an initially very low value on adding pyridine (to 8×10^{-5} M) to a pyridine-free gold sol.[3] We have been unable to repeat this experiment with the copper sols, since aggregation was too fast on adding pyridine (to 1×10^{-4} M) to a pyridine-free copper sol, the change in the extinction spectrum being already considerable 30 s after adding the pyridine. However, we have measured the evolution of the pyridine SER signal (1010-cm^{-1} band) during the formation of a copper–pyridine sol, and Figure 10 shows such a measurement made on the same developing sol as Figure 1b. As may be seen by reference to Figure 1, the SER signal becomes detectable after ca. 6 min, at the stage at which aggregation first becomes apparent in the extinction spectrum, as would be consistent with the notion that some aggregation is essential for the observation of intense SER scattering. The small maximum in the SER intensity in Figure 10 after 7–8 min was reproduced in each of several runs, but this maximum is not associated with any noticable feature in the evolution of the absorption, and we are unable to account for its origin.

In the earlier work on aggregated silver and gold colloids it was shown that there is a similarity between the excitation profiles for SER scattering and the colloid extinction spectra.[3] For these colloids the aggregate plasma resonances were relatively sharp, and it was observed that the SER excitation profile peaked at a wavelength close to the long wavelength extinction maximum of the sols.[2,3] It was further shown[3] that for the aggregated colloids the excitation profile could be calculated from the extinction profile by the approximate relationship

$$I = \text{constant} \times \left[\frac{|\epsilon_0|^2 |\epsilon_R|^2}{\nu_0 \nu_R (\epsilon_2)_0 (\epsilon_2)_R} \right] A_0 A_R \qquad (1)$$

where A_0 and A_R are the fractional absorptions and $\epsilon_0 = (\epsilon_1)_0 + i(\epsilon_2)_0$ and $\epsilon_R = (\epsilon_1)_R + i(\epsilon_2)_R$ are the metal dielectric functions at the excitation and Raman scattered frequencies ν_0 and ν_R, respectively, and I is the Raman intensity.[4] In the case of the copper sols there is no obvious similarity between the extinction spectrum and the SER excitation profile (Figure 3). The plasma resonance of the aggregates is quite broad, giving a rather flat extinction extending out into the far red, whereas the excitation profile rises steeply from near 600 nm into the infrared. However, Figure 3 includes the excitation profile calculated from the extinction spectrum by means of eq 1, and again the agreement with the experimental profile is seen to be very satisfactory bearing in mind the polydisperse nature of the sol. Because of the flatness of the extinction spectrum, it emerges from eq 1 that the steep rise in the SER profile is almost entirely a consequence of the rise in $|\epsilon|^2$ for copper toward the red, and the same is probably true for the excitation profiles for roughened bulk copper surfaces, which also rise steeply to the red.[5,6,8]

The agreement between the measured excitation profile and that predicted from eq 1 is perhaps somewhat surprising since the expression was originally derived for island films.[4] In that case, the very close proximity of the neighboring islands leads to a strong electromagnetic coupling between the islands causing the spectral shape of the absorption to be uniform over the whole film. Thus, the measured absorption can be used adequately to approximate the field enhancement at both the excitation and Raman scattered frequency. In contrast, both the absorption spectra and the dynamic light scattering results suggest that the aggregated copper sols are quite polydisperse in nature. Furthermore, the individual colloids are rather widely separated in the solution. Thus, the fact that the simple expression in eq 1 gives such good agreement presumably reflects the fact that the frequency dependence of the excitation profile is dominated by the very rapid rise in $|\epsilon_0|^2|\epsilon_R|^2$ at increasing wavelengths.

The relatively weak Raman bands of pyridine have not been reported in previous work on metal colloids or on copper surfaces, though they have been observed for pyridine adsorbed at silver electrodes. The relative intensities of these modes are of interest as a probe of the orientation of the adsorbed molecule, as is discussed elsewhere.[19] As Table I shows, the b_2 modes of adsorbed pyridine are particularly weak when compared to these modes of pyridine in solution, and it is clear that these modes are the least enhanced. Since the relevant polarizability tensor component for b_2 Raman scattering is α_{xz}, where x and z define the molecule plane, it follows from the electromagnetic enhancement model of the SER effect that the average electromagnetic field enhancement is least in the field components which lie in the plane of the molecule. Since from the electromagnetic boundry conditions the enhancement is least for the field components parallel to the surface, it is thus concluded that the molecule is adsorbed flat-on to the surfaces. This orientation of adsorbed pyridine has also been reported for the Cu(110)–vacuum interface at room temperature (2 langmuirs exposure) from angle-resolved photoemission data.[20] It must be emphasized, however, that other nonelectromagnetic enhancement models have been neglected in reaching this conclusion from the SERS intensities regarding the adsorbed pyridine orientation, and in view of the unknown effect of contributions from these other mechanisms on the SER band relative intensities this orientation cannot

(19) J. A. Creighton, *Surf. Sci.*, **124**, 209 (1983).
(20) B. J. Bandy, D. R. Lloyd, and N. V. Richardson, *Surf. Sci.*, **89**, 344 (1979).
(21) H. D. Stidham and D. P. DiLella, *J. Raman Spectrosc.*, **9**, 247 (1980).

be regarded as firmly established.

Consideration of the scattering tensor within the electromagnetic enhancement model also may provide an explanation of the variation in the relative intensities of some of the modes on changing from 647.1- to 752.5-nm excitation (see Table I). Considering first the a_1 modes, all three diagonal tensor elements α_{xx}, α_{yy}, and α_{zz} contribute to Raman scattering by a_1 modes, and since the relative magnitudes of these elements may differ for different modes, the Raman intensities may respond differently to changes in the relative size of the electromagnetic field components perpendicular and parallel to the surface. On changing from 647.1- to 752.5-nm excitation the perpendicular field component at any point of the surface increases relative to the parallel component, due to the increase in $|\epsilon|$ for copper with increase in wavelength, and thus a_1 modes for which α_{xx}^2, $\alpha_{zz}^2 > \alpha_{yy}^2$ are expected to decrease in SER intensity relative to modes for which α_{xx}^2, $\alpha_{zz}^2 < \alpha_{yy}^2$. As far as we are aware there is no information on the magnitude of the components of α for the various pyridine modes, but there are certainly large differences in the diagonal components of α for the a_1 modes of pyridine in aqueous solution, as is shown by the difference in the solution a_1 band depolarization ratios (see Table I), and thus changes in the SER relative intensities of a_1 bands with change in excitation wavelength are entirely consistent with the electromagnetic enhancement model. The increase in the perpendicular field relative to the parallel field component with increase in wavelength also accounts for the changes in the relative intensities of the non-a_1 modes as the wavelength is increased. Thus as Table I shows, the b_2 mode at 1150 cm^{-1}, which involves only field components parallel to the surface (assuming flat-on adsorption of pyridine), diminishes considerably in intensity relative to the 1010-cm^{-1} a_1 mode on changing from 647.1- to 752.5-nm excitation, while the a_2 and b_1 modes, which involve both parallel and perpendicular surface fields, are less diminished for this wavelength change. In fact, these results are also quite consistent with eq 1 if the factors of $|\epsilon|_0^2$ and $|\epsilon|_R^2$, which arise from the boundary conditions for fields normal to the surface, are no longer included, to reflect the effects of the field parallel to the surface.

In conclusion we present here the first report of surface-enhanced Raman scattering by copper colloids. The results are consistent with the conclusions of earlier work on silver and gold colloids, and thus the copper colloids which show intense SER scattering are shown to be partially aggregated, as is demonstrated in situ by dynamic light scattering. We show that the excitation profile is related to the measured absorption profile, and demonstrate that the increase in $|\epsilon|^2$ toward longer wavelengths makes an important contribution to the profile. Thus the excitation profile is consistent with the electromagnetic enhancement model of the SER effect. This model is shown also to enable the relative enhancement and intensity vs. wavelength dependence for modes of different symmetry to be interpreted to suggest the adsorbate orientation at the surface. Some preliminary measurements to illustrate the use of SER spectroscopy to investigate competitive adsorption on copper colloids are also presented.

Registry No. Cu, 7440-50-8; Ph_2S, 139-66-2; PhSH, 108-98-5; pyridine, 110-86-1; 4,4'-bipyridine, 553-26-4.

Radiationless Transitions in Excited Electronic States of the Benzene Cation in the Gas Phase

O. Braitbart,† E. Castellucci,‡ G. Dujardin, and S. Leach*

Laboratoire de Photophysique Moléculaire du C.N.R.S.,§ Bâtiment 213, Université Paris-Sud, 91405 Orsay Cédex, France
(Received: February 28, 1983)

Emission from electronic excited states of the benzene-h_6 ($Bz(h_6)$) and benzene-d_6 ($Bz(d_6)$) gas-phase cations was searched for by using the PIFCO technique in which mass-selected photoion–fluorescence photon coincidences are counted. The maximum fluorescence efficiency was found to be 4×10^{-5} for benzene ions produced with He I 584-Å excitation. From the derived maximum quantum yields and an estimate of the fluorescent decay rate, the nonradiative relaxation rate k_{nr} of electronic excited states of the benzene cation was determined to be greater than 5×10^{12} s^{-1} for the $\tilde{C}^2A_{2u}$ state and greater than 8×10^{10} s^{-1} for the $\tilde{B}^2E_{2g}$ state. The absence of an observed deuterium effect on the fluorescence efficiency is consistent with these high k_{nr} rates. A discussion is given of possible relaxation pathways of the excited states; for the $\tilde{C}$ and $\tilde{B}$ states it is shown that relaxation could take place by $\tilde{C} \rightsquigarrow \tilde{B} \rightsquigarrow \tilde{X}$ and $\tilde{C} \rightsquigarrow \tilde{X}$ interelectronic couplings and by isomerization to Dewar benzene and/or benzvalene cations.

Introduction

The evolution and fate of the benzene cation in its excited electronic states has been the subject of much experimental work, discussion, and conjecture. In a recent publication, Rosenstock et al.[1] have presented a critical review of our understanding of the fragmentation behavior of electronically excited $C_6H_6^+$ systems. The present work mainly concerns the dynamics of electronically excited states of the gas-phase benzene cation at energies below the lowest dissociation limit. This dynamics is intimately linked to the question of whether optical emission occurs

† Permanent address: Racah Institute of Physics, Hebrew University of Jerusalem, Israel.

‡ Permanent address: Istituto di Chimica Fisica, Università di Firenze, Italy.

§ Laboratoire associé à l'Université Paris-Sud.

(1) H. M. Rosenstock, J. Dannacher, and J. F. Liebman, *Radiat. Phys. Chem.*, **20**, 7 (1982).

0022-3654/83/2087-4799$01.50/0